Iraqi J. Laser, Part A, Vol.17, pp.33-39 (2018)

IRAQI JOURNAL OF LASER

All Fiber Chemical Liquids Refractive Index Sensor Based on Multimode Interference

Saif A. Mohammed and **Abdul H. Al-Janabi**

Institute of laser for postgraduate studies, University of Baghdad, Baghdad, Iraq
eng.saifakeel@gmail.com

(Received 15 October 2017; accepted 24 December 2017)

Abstract: A simple all optical fiber sensor based on multimode interference (MMI) for chemical liquids sensing was designed and fabricated. A segment of coreless fiber (CF) was spliced between two single mode fibers to buildup single mode-coreless-single mode (SCS) structure. Broadband source and optical signal analyzer were connected to the ends of SCS structure. De-ionized water, acetone, and n-hexane were used to test the performance of the sensor. Two influence factors on the sensitivity namely the length and the diameter of the CF were investigated. The obtained maximum sensitivity was at n-hexane at 340.89 nm/RIU (at a wavelength resolution of the optical spectrum analyzer of 0.02 nm) when the diameter of the CF reduced from 125 µm to 60 µm and the length with 2 cm.

Keywords: refractive index sensing, single mode-coreless-single mode fiber structure, coreless fiber, Multimode interference.

Introduction:

All optical fiber sensors are based on Multimode interference (MMI) that have potential applications in many fields like manufacturing industry [1], environmental monitoring [2, 3], and biochemical reactions [4, 5]. Comparing with another sensors, all fiber sensor has many attractive advantages such as easy to fabricate, low cost, electromagnetic immunity, compact, and high sensitivity [6-8]. Different structures of all fiber sensor were demonstrated such as a photonic crystal fiber (PCF) [9], fiber Bragg grating (FBG) [10], a Mach-Zehnder interferometer (MZI) [11], single-mode-multimode-single-mode fiber structures (SMS) [12], and single-mode-coreless-single-mode fiber structures [13]. Recently, the single mode-coreless-single mode (SCS) fiber structures have been designed to sense temperature [14], refractive index (RI) [15], chemical concentration [16], and magnetic field [17]. The essential sensing principle is based on the multimode interference within the coreless fiber (CF). The sensitivity of these structures depends on the difference of response to ambient variation between the involved modes where the surrounding refractive index acts as cladding refractive index of coreless fiber. Recently, many efforts have been made to improve the coreless fiber based sensor sensitivity. X. Zhou et al [18] used gold film deposited at CF end to improve the sensitivity within the refractive index RI range from 1.33-1.38. Nevertheless, this sensor structure is considered complex and expensive. The influence of the length and the outer diameter of CF have been studied by many researchers to enhance the sensitivity of the SCS fiber structure sensor. Z. Liu et al used

homemade CF with a diameter of 104 µm to build up a sensor inside fiber laser cavity [19]. The structure showed a red shift with maximum sensitivity at 131.64 nm/RIU. The sensitivity has been improved from 214.24 nm/RIU when CF diameter reduced to 80 µm at RI range from 1.33-1.37 using CF spliced between two segments of FBG by C. Zhang et al [20], had built a dual sensing sensor for measuring RI and temperature however it is considered expensive structure. In this work, an RI sensor has been designed and fabricated to measure the change in RI of liquid based on MMI. The all-fiber SCS structure is formed by sandwiching a short length of CF between two standard SMFs. In order to improve the measurement sensitivity, the CF was etched deeply by acid solution. The influence of CF length and diameter on sensitivity were tested using three different CF lengths and four different diameters.

Experimental work and principles:

Principles and Operations:

Figure 1 shows the schematic of proposed all fiber SCS structure sensor. This sensor was fabricated by splicing three different lengths of CF with outer diameter at 125 µm between two single mode fibers (Corning SMF-28) to fabricate the three SCS structures with different lengths to study the influence of the length on the sensitivity. The CF segment acts as sensing element. The CF is an all-silica fiber with large diameter (125 µm) and the surrounding air acts as its cladding. The mode-mismatch splicing technique was employed for the implementation of the all-fiber SCS structure sensor. Light propagating along the SMF has a Gaussian field intensity distribution (fundamental mode) as it is confined into very small core diameter (9 µm). The mode-mismatch between SMF and CF allows the fundamental mode in SMF to couple into a CF. Then, the fundamental mode begins to diffract within the CF.

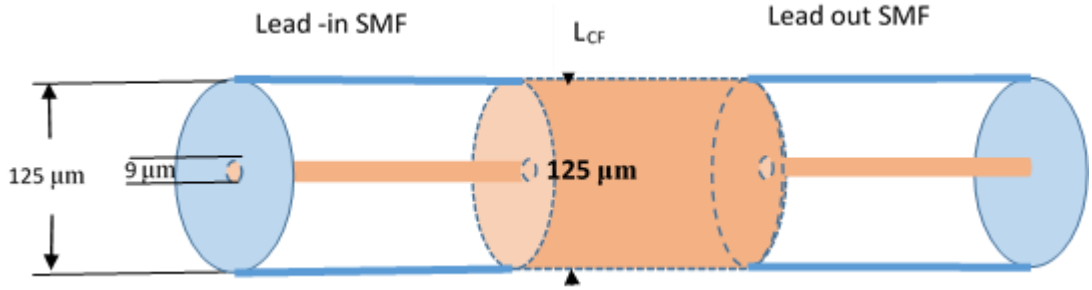

Fig. 1: Schematic diagram of the proposed all-fiber SCS structure sensor.

High order modes are excited and propagated independently along the CF section. These high order modes are interfered with each other and appeared as a superposition of their mode field. Generally these high order modes produce a complicated field distribution due to multimode interferences (MMI) effect [21]. When the diameter of the CF segment is reduced, the evanescent waves (EW) of the light in this CF penetrates further into the outer surrounding medium (OSM), thus the interaction between the EW and OSM is increased thus enhances the sensitivity [22]. The length and the diameter of the CF are key parameters in the design of such sensor. According to MMI theory, the length of the CF can be given by [21, 23, 24 and [25]:

$$L_{CF} = p\left(\frac{3L_{\pi}}{4}\right) \quad \text{with p=0, 1, 2,} \qquad (1)$$

Where the parameter p denotes the constructive interference number (self-imaging number). Such constructive interference occurs at periodic intervals defined by p, (p =0, 1, 2 …), at these lengths the formed images show a profile of a narrow width and a high amplitude, and L_{π} is the beat length and can be expressed as

$$L_{\pi} = \frac{4n_{CF}D_{CF}^2}{3\lambda_0} \qquad (2)$$

Thus, the peak spectral response of this CF caused by self-imaging effect can be expressed as

$$\lambda_o = p\left(\frac{n_{CF}D_{CF}^2}{L_{CF}}\right) \qquad (3)$$

Here n_{CF} and D_{CF} are correspond to the effective (RI) and the diameter of CF section, respectively.

Sensor fabrication and characterization:

Three SCS structures with three different lengths of CF (Thorlabs Inc.) were fabricated using automatic splicing conditions. The SMF (Coring SMF-28) sections have 1.451 and 1.444 refractive indices for the core and cladding, respectively. The core and the cladding diameters of the SMF sections were 9 µm and 125 µm, respectively. The CF has refractive index of 1.444 at 1550 nm and diameter of 125 µm. Therefore, the same refractive indices of 1.444 for the SMF clad and the CF reserves the optical homogeneity. The fabrications process was as follow: firstly, CF with 125 µm diameter was cleaved according to a certain length range and both ends are spliced with two standard SMFs using a standard fusion splicer (Fujikura FSM-60S) with automatic mode to form SMF-CF-SMF (SCS) structure as shown in the Figure 2.

Fig. 2. The splicing region between SMF and CF using automatic splicing mode

Then, the fabricated SCS structure was fixed in the quartz material U-shape groove. The test indexed liquids were poured inside the U-shaped groove to test the change in refractive indices.

The SCS structure is then tightly stretched and fixed by two bare fiber holders placed on 3-D (xyz) mount stage (Newport). Both ends of the U-shape groove were sealed. These steps were repeated with the three different lengths (2, 4 and 6 cm) of SCS structure.

One of the techniques used to further enhance the sensitivity of the SCS structure is by decreasing the CF diameter. Our target is to reach 60 µm in diameter. This was carried out by etching the CF at 4 cm length with acid solution post SCS structure fabrication. Then, the fabricated SCS structure was fixed in the quartz material U-shape groove. This groove was used to contain the etching solution and to test the change in refractive index. The SCS is then also tightly stretched and fixed by two bare fiber holders placed on 3-D (xyz) mount stage (Newport). Both ends of the U-shape groove were sealed. The CF of selected length of 4 cm of the SCS was etched in the hydrofluoric solution (HF) ~ 40%. This resulted in a decrease of CF diameter in steps from 125 µm to 100, 80, and 60 µm.

The experimental setup of the proposed all-fiber SCS is depicted in Figure 3

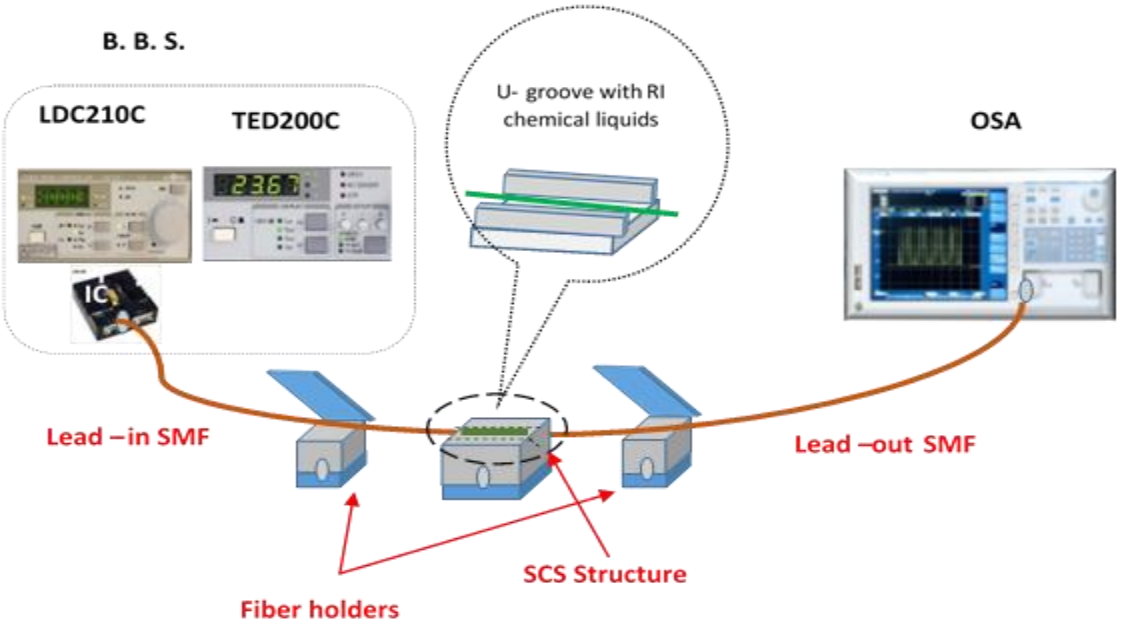

Fig. 3. Experimental setup of all-fiber SCS fiber structure sensor

The transmission measurement setup for the proposed sensor was carried out using a pump broadband source (Thorlabs) with wavelength range 1500-1600 nm spliced to one end of the SCS structure and an optical spectrum analyzer (YOKOGAWA AQ6370C OSA) with resolution of 0.02 nm spliced to the other end. The SCS structure is fixed using bare fiber holder to avoid the impact of fiber bending or strain on the spectral transmission characteristics of all-fiber sensor.

Results and Discussion

The proposed SCS structures with (2, 4, and 6) cm of CF length have been immersed in deionized water (n= 1.333), Acetone (n= 1.3514), and n-hexane (n=1.370). These liquids act as a cladding for CF instead of air. The resulted wavelength shift and sensitivity were recorded using OSA. The above procedures was repeated with 2 cm and 4cm of CF length.

The wavelength dips were shifted towards red shift when the refractive index increased from 1 in air to 1.3751 in n-hexane as shown in Figures (4, 5, and 6).

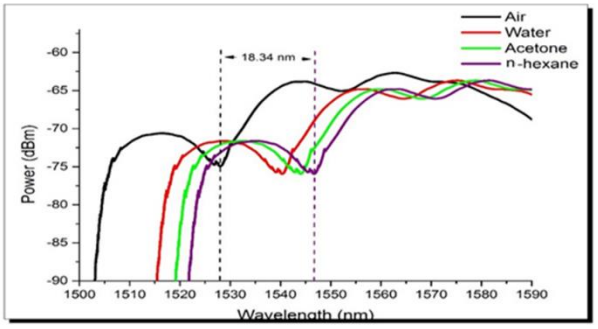

Fig. 4. Experimental output power versus wavelengths for 2 cm length of CF

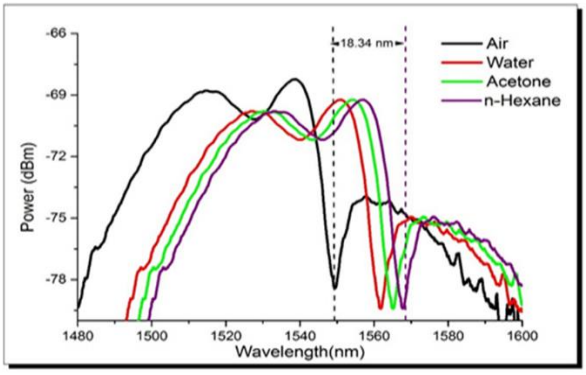

Fig. 5. Experimental output power versus wavelengths for 4 cm length of CF

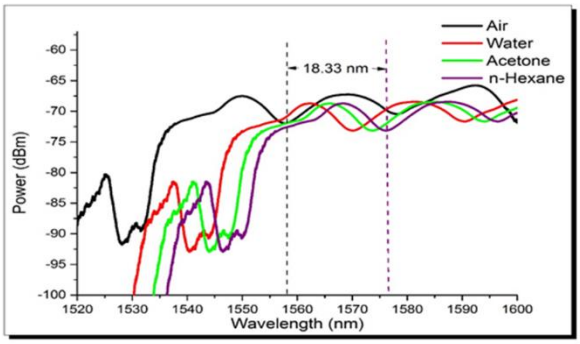

Fig. 6. Experimental output power versus wavelengths for 6 cm length of CF

The relationship between the variations in CF length with wavelength shift is depicted Figure 7.

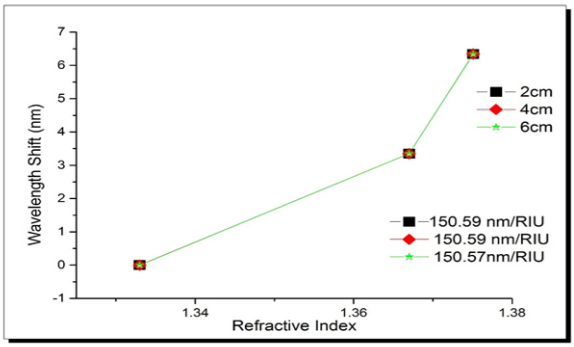

Fig. 7. Wavelength Shift (nm) as a function of different CF lengths at fixed CF diameter 125 µm

The sensitivity and wavelength have no noticeable change with the variation of the length of the CF when outer diameter of CF was fixed at 125 µm. This might be due to the self-imaging effect in MMI.

To examine the role of the CF diameter on the sensitivity, the SCS structure with 4 cm of the CF length has been etched to 100 µm. Then the SCS structure has been immersed in deionized water, acetone, and n-hexane respectively. The resulted wavelength shift and sensitivity were recorded. The above procedures were repeated with 80 µm, and 60 µm, of CF diameter.

From Figures (5, 8, 9, and 10), the wavelength dips have red shift when refractive index increased from 1 in air to 1.3751 in hexane. The sensitivity increased from 150.831 nm/RIU to 340.89 nm/RIU when diameter of CF decreased from 125 µm to 60 µm with fixed CF length at 4 cm as shown in Figure 12. A remarkable enhancement is achieved compared to a recently published work [20]. Sensitivity enhancement might be due to that the decrease in the diameter allows more interaction of evanescent wave with

surrounding refractive index forming the self-imaging effect in MMI [26].

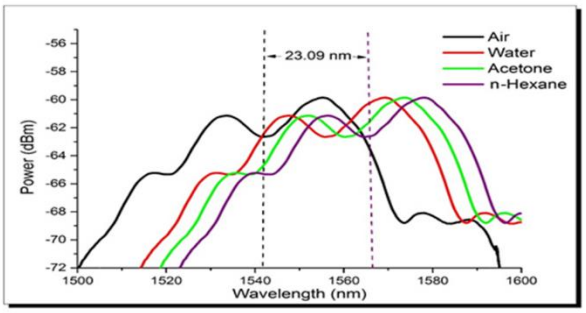

Fig. 8. Experimental output power versus wavelengths for 100 µm diameter of CF

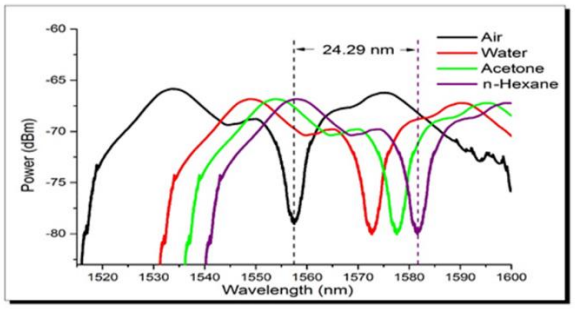

Fig.9. Experimental output power versus wavelengths for 80 µm diameter of CF

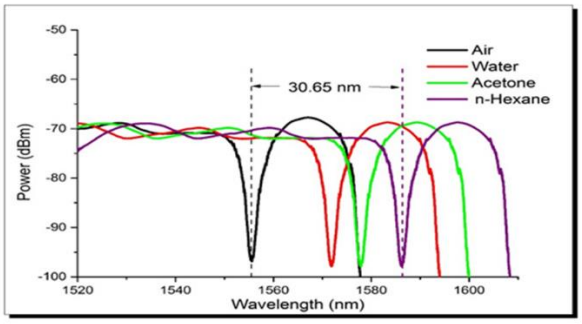

Fig. 10. Experimental output power versus wavelengths for 60 µm diameter of CF

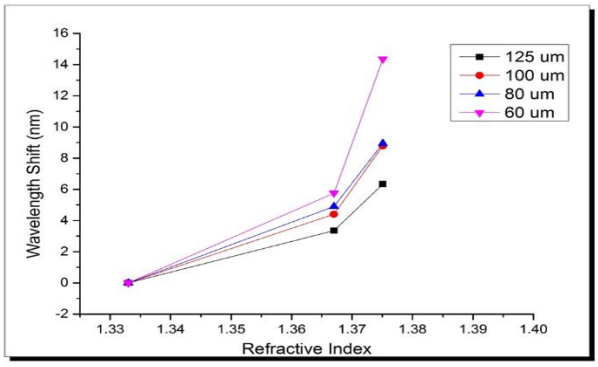

Fig. 11. Wavelength Shift (nm) as a function of different CF Diameters

The change in refractive index due to the change the effective refractive index (n_{eff}) of the interfering cladding mode propagating in the CF the modulation of the (n_{eff}) occurs which accordingly lead to change the position of the interference pattern[25]. Also the maximum shift increase depends on the etched value of the CF diameter [13].

Conclusions

A highly sensitive concentration / RI sensor based on etching (SCS) fiber structure has been demonstrated experimentally. The influence of the CF length and diameter was the key control parameter to optimize the sensor performance. The length of CF has no noticeable effect on the RI sensitivity when CF diameter is 125 µm. The obtained sensitivity has been improved when diameter of CF reduced by etching from 125 µm to 60µm with maximum wavelength shift at 30.89 nm. The maximum obtained sensitivity is at 340.85 nm/RIU when diameter of CF decreased to 60 µm with chemicals liquids. The sensitivity was increased by 12% compared with the previous work in [20] when the CF is used instead of MMF. The results showed that the sensitivity can be enhanced by shortening the length of CF when CF diameter reduced to 60 µm within the experiment's conditions. This sensor has many advantage such as high sensitivity in real time, an evident central wavelength shift, low cost, ease in fabrication, small size and compactness.

References

[1] C. J. Brooks, A. P. Knights, and P. E. Jessop, "Vertically-integrated multimode interferometer coupler for 3D photonic circuits in SOI", Optics Express, Vol. 19, No. 4, pp. 2916-2921, (2011).

[2] Y. Chen, Y. Wang, R. Chen, W. Yang, H. Liu, T. Liu, and Q. Han, "A Hybrid Multimode Interference Structure-Based Refractive Index and Temperature Fiber Sensor", IEEE Sensors Journal, Vol. 16, No.2, pp. 331-335, (2016).

[3] D. Watanabe, H. Fukano, and S. Taue, "High sensitivity optical-fiber temperature sensor with solid cladding material based on multimode interference", proceeding of Opto-Electronics and Communications Conference (OECC), 28 June-2 July, (2015).

[4] N. H. Wan, F. Meng, T. Schröder, R. Shiue, E. H. Chen, and D, Englund, "High-resolution optical spectroscopy using multimode interference in a compact tapered fibre", Nature

Communications, ***6***, Article number: 7762, (2015).
[5] M. Mayeh, J. Viegas, P. Srinivasan, P. Marques, J. L. Santos, E. G. Johnson, and F. Farahi, "Design and Fabrication of Slotted Multimode Interference Devices for Chemical and Biological Sensing", Journal of Sensors, 2009, Article ID: 470175, pp. 1-11, (2009).
[6] J. E. Antonio-Lopez, D. A. May-Arrioja, and P. LiKamWa, "Fiber-Optic Liquid Level Sensor", IEEE Photonics Technology Letters, ***23***, No.23, pp. 1826-1826, (2011).
[7] E. E. Antúnez-Cerón, M. A. Basurto-Pensado, A. R. Mejía-Aranda, R. J. Romero, J. J. Sánchez-Mondragón, H. H. Cerecedo-Núñez, and A. Ochoa-Zezzati, "Estimation of LiBr-H2O Using Multimode Interference (MMI)", Journal of Applied Research and Technology, ***12***, 1, pp. 41-44, (2014).
[8] W. S. Mohammed and P. W. E. Smith,"All-fiber multimode interference bandpass filter", Optics Letters, ***31***, No.17, pp. 2547-2549, (2006).
[9] S. Qiu,Y. Chen, F. Xu, and Y. Lu, "Temperature sensor based on an isopropanol-sealed photonic crystal fiber in-line interferometer with enhanced refractive index sensitivity", Optics Letters, ***37***, No. 5, pp. 863-865, (2012).
[10] C. Zhang, S. Xu, J. Zhao, H. Li, H. Bai, and C. Miao, "Differential Intensity Modulation Refractometer Based on SNS Structure Cascaded Two FBGs", IEEE Photonics Journal, ***9***, No. 3, ID 7103008, pp. 1-8, (2017).
[11] Z. Liu, Z. Tan, B. Yin, Y. Bai, and S. Jian, "Refractive index sensing characterization of a singlemode–claddingless–singlemode fiber structure based fiber ring cavity laser", Optics Express, ***22***, No. 5, pp. 5037-5042, (2014).
[12] Y. Zhaoa, L. Cai, X. Li, F. Meng, and Z. Zhao," Investigation of the high sensitivity RI sensor based on SMS fiber structure", Sensors and Actuators, A, ***205***, pp. 186-190, (2014).
[13] L. Ma, Y. Qi, Z. Kang, and S. Jian, "All-Fiber Strain and Curvature Sensor Based on No-Core Fiber". IEEE Sensors Journal, ***14***, No. 5, pp. 1514-1517, (2014).
[14] P. Hu, Z. Chen, M. Yang, J. Yang, and C. Zhong, "Highly sensitive liquid-sealed multimode fiber interferometrictemperature sensor", Sensors and Actuators, A, ***223***, pp. 114–118, (2015).
[15] Y. Li, Z .Liu, and S. Jian, "Multimode Interference Refractive Index Sensor Based on Coreless Fiber", Photonic Sensors, ***4***, No.1, pp. 21-27, (2014).
[16] Z. Wu, X. Yu, E. Gu, Z. Kong, and W. Li, "Characteristics analysis of chemical concentration sensor based on three-layer FBG. Optics and Photonics Journal, ***3***, pp. 268-271, (2013).
[17] H. Wang, S. Pu, N. Wang, S. Dong, and J. Huang, "Magnetic field sensing based on singlemode–multimode–singlemode fiber structures using magnetic fluids as cladding" Optics Letters, ***38***, No. 19, pp. 3765-3765, (2013).
[18] J. Wang, and J. Tang "Photonic crystal fiber Mach-Zehnder interferometer for refractive index sensing". Sensor ***12***: 2983-2995 (2012).
[19] Z. Liu, Z. Tan, B. Yin, Y. Bai, and S. Jian, "Refractive index sensing characterization of a singlemode–claddingless–singlemode fiber structure based fiber ring cavity laser", Optics Express, ***22***, No. 5, pp. 5037-5042, (2014).
[20] C. Zhang , S. Xu, J. Zhao, H. Li, H. Bai, C. Miao, "Intensity-modulated refractive index sensor with anti-light source fluctuation based on no-core fiber filter", Optics and Laser Technology, ***97***, pp. 358-363, (2017).
[21] W.A. Khaleel, and A. H. Al-Janabi, "High-sensitivity sucrose erbium-doped fiber ring laser sensor". Optical Engineering, ***56***, No. 2, pp. 0261161-0261166, (2017).
[22] Ji. Lou, L. Tong, and Z. Ye, "Modeling of silica nanowires for optical sensing", Optics Express, ***13***, No. 6, pp. 2135-2140, (2005).
[23] X. Lan, J. Huang, Q. Han, T. Wei, Z. Gao, H. Jiang, J. Dong, and H. Xiao, "Fiber ring laser interrogated zeolite-coated singlemode-multimode-singlemode structure for trace chemical detection". Optics Letters, ***37***, No. 11, pp. 1998-2000, (2012).
[24] R. Oliveira, T. H. R. Marques, L. Bilro, R. Nogueira, "Multiparameter POF Sensing based on Multimode Interference and Fiber Bragg Grating", Journal of Ligthwave Technology, ***35***, No. 1, pp. 3-9, (2017).
[25] L. Huang, G. Lin, M. Fu, H. Sheng, H. Sun, and W. Liu, " A Refractive-index Fiber Sensor by Using No-Core Fibers", In Proceedings of the 2013 IEEE International Symposium on Next-generation Electronics, Kaohsiung, Taiwan, 25 February, pp. 100-102, (2013).
[26] J. Zhao, J. Wang, C. Zhang, C. Guo, H. Bai, W. Xu, L. Chen, and C. Miao, "Refractive Index Fiber Laser Sensor by Using Tunable Filter Based on No-Core Fiber", IEEE Sensors Journal, ***8***, No. 5,ID 6805008, pp. 1-8, (2016).

تصميم متحسس من الالياف البصرية بالكامل لتحسس تغير معامل انكسار السوائل الكيميائية والمعتمد على مبدأ تداخل الانماط المتعدد

سيف عقيل محمد عبد الهادي الجنابي

معهد الليزر للدراسات العليا ، جامعة بغداد ، العراق

الخلاصة : تم تصميم وبناء متحسس بسيط من الليف البصري بالكامل والمستند على مبدأ تداخل الانماط المتعدد لتحسس السوائل الكيميائية. قطعة من الليف خالي القلب تم ربطها بين قطعتين من الليف احادي النمط لبناء التركيب احادي النمط - خالي القلب - احادي النمط. تم ربط مصدر ضوئي واسع الطيف مع محلل الطيف الضوئي عند نهايتي التركيب احادي النمط - خالي القلب - احادي النمط. تم استعمال ماء منزوع الايونات, واسيتون, و n- الهكسان لغرض فحص اداء هذا المتحسس. تم التحقق من تأثير اثنين من العوامل على حساسية المتحسس وهي طول الليف خالي القلب وقطره. وكانت الحساسية القصوى التي تم الحصول عليها في n- الهكسان في 340.89 نانومتر \ وحدة معامل الانكسار (عند قرار الطول الموجي لمحلل الطيف الضوئي من 0.02 نانومتر) عندما انخفض قطر الليف خالي القلب من 125 ميكرون إلى 60 ميكرون عند طول 2 سنتميتر.